Behavioral/Cognitive

Age-Related Changes in 1/*f* Neural Electrophysiological Noise

Bradley Voytek,[1] Mark A. Kramer,[3] John Case,[4] Kyle Q. Lepage,[3] Zechari R. Tempesta,[1] Robert T. Knight,[4,5] and Adam Gazzaley[1,2]

Departments of [1]Neurology and [2]Physiology and Psychiatry and UCSF Center for Integrative Neuroscience, University of California, San Francisco, California 94158, [3]Department of Mathematics and Statistics, Boston University, Boston, Massachusetts 02215, and [4]Helen Wills Neuroscience Institute and [5]Department of Psychology, University of California, Berkeley, California 94720

Aging is associated with performance decrements across multiple cognitive domains. The neural noise hypothesis, a dominant view of the basis of this decline, posits that aging is accompanied by an increase in spontaneous, noisy baseline neural activity. Here we analyze data from two different groups of human subjects: intracranial electrocorticography from 15 participants over a 38 year age range (15–53 years) and scalp EEG data from healthy younger (20–30 years) and older (60–70 years) adults to test the neural noise hypothesis from a 1/*f* noise perspective. Many natural phenomena, including electrophysiology, are characterized by 1/*f* noise. The defining characteristic of 1/*f* is that the power of the signal frequency content decreases rapidly as a function of the frequency (f) itself. The slope of this decay, the noise exponent (χ), is often < -1 for electrophysiological data and has been shown to approach white noise (defined as $\chi = 0$) with increasing task difficulty. We observed, in both electrophysiological datasets, that aging is associated with a flatter (more noisy) 1/*f* power spectral density, even at rest, and that visual cortical 1/*f* noise statistically mediates age-related impairments in visual working memory. These results provide electrophysiological support for the neural noise hypothesis of aging.

Key words: **1/*f*; electrocorticography; EEG; neural noise; phase/amplitude coupling; working memory**

Significance Statement

Understanding the neurobiological origins of age-related cognitive decline is of critical scientific, medical, and public health importance, especially considering the rapid aging of the world's population. We find, in two separate human studies, that 1/*f* electrophysiological noise increases with aging. In addition, we observe that this age-related 1/*f* noise statistically mediates age-related working memory decline. These results significantly add to this understanding and contextualize a long-standing problem in cognition by encapsulating age-related cognitive decline within a neurocomputational model of 1/*f* noise-induced deficits in neural communication.

Introduction

Communication is more efficient in the presence of less noise (Shannon, 1948), whether that communication is between friends in a crowded room or between a radio transmitter and receiver tuned to a favorite station. As we age, we are faced with the likelihood that our cognitive faculties will decline (Gazzaley et al., 2007; Salthouse, 2010), our neural and behavioral response times (RTs) will be slower and more variable (Salthouse, 2010), our memories less certain (Nyberg et al., 2012), and our attention less focused (Gazzaley et al., 2005). The neural noise hypothesis is an attempt to account for these age-related changes and states that, with aging, the effective signal to noise of neural communication diminishes (Cremer and Zeef, 1987). Reduced signal to noise may arise as a function of increased spontaneous/baseline neural spiking activity (Hong and Rebec, 2012), which in turn disrupts the fidelity of neural communication, resulting in cognitive impairments (Voytek and Knight, 2015).

The definition of noise adopted here derives from signal processing wherein time-series data are characterized by the shape of their frequency domain representation. A line in semi-log or log-

Received June 9, 2014; revised Aug. 20, 2015; accepted Aug. 22, 2015.

Author contributions: B.V., R.T.K., and A.G. designed research; B.V. performed research; B.V., M.A.K., K.Q.L., and Z.R.T. contributed unpublished reagents/analytic tools; B.V., J.C., K.Q.L., and Z.R.T. analyzed data; B.V., M.A.K., J.C., R.T.K., and A.G. wrote the paper.

B.V. was supported by a National Institutes of Health Institutional Research and Academic Career Development Award (GM081266) and a University of California Presidential Postdoctoral Fellowship. B.V. and R.T.K. were supported by the National Institute of Neurological Disorders and Stroke and the Nielsen Corporation. A.G. was supported by the National Institute on Aging. M.A.K. was supported by National Institute of Neurological Disorders and Stroke Award R01NS072023. We thank Edward Chang, Nathan Crone, and Josef Parvizi for patient care and data collection assistance.

The authors declare no competing financial interests.

Correspondence should be addressed to Dr. Bradley Voytek, Department of Cognitive Science, UC San Diego, 9500 Gilman Dr., La Jolla, CA 92093-0515. E-mail: bradley.voytek@gmail.com.

DOI:10.1523/JNEUROSCI.2332-14.2015

 0270-6474/15/3513257-09$15.00/0

log space can approximate this "1/*f* noise" representation. The slope of this line is the noise exponent where white noise, which is serially uncorrelated in the time domain, has a flat spectral slope of 0. Electrophysiological data, in contrast, often have a negative slope (Miller et al., 2009a; He et al., 2010; He, 2014). This slope has been shown to change during sleep versus waking (Freeman and Zhai, 2009) and with behavioral state (Podvalny et al., 2015). One possible mechanism underlying this change is an alteration in the underlying population spiking statistics (Gao, 2015; Voytek and Knight, 2015). If the neuronal population is highly correlated (a large number of spikes all occur relatively simultaneously, with few aberrant units spiking at times different from the population mode), then the aggregate local field potential (LFP) 1/*f* slope will be more negative. As the units within the population spike relatively asynchronously, the LFP 1/*f* slope will be flatter (Usher et al., 1995; Pozzorini et al., 2013; Podvalny et al., 2015; Voytek and Knight, 2015). Within this framework, age-related increases in neural noise would result in desynchronized spiking activity, reflected by a flatter power spectrum (Hanggi and Jung, 1995; Bédard et al., 2006; Sosnoff and Newell, 2011; Hong and Rebec, 2012; Podvalny et al., 2015).

The second hypothesized consequence of increased neural noise is a decoupling of population spiking activity from the ongoing low-frequency oscillatory neural field (Tort et al., 2010; Lepage et al., 2011; Voytek and Knight, 2015). Empirical observations show that the phase of low-frequency oscillations, such as theta (4–8 Hz) and alpha (8–12 Hz), is comodulated with the amplitude of high gamma power (80–150 Hz) (Canolty et al., 2006; Osipova et al., 2008; Voytek et al., 2010a). The low-frequency oscillatory activity is thought to bias neural activity dependent upon the ongoing oscillation phase (Canolty et al., 2006; Voytek et al., 2010a) analogous to spike/phase coupling (Fries, 2005; Montemurro et al., 2008; Fröhlich and Mccormick, 2010), and is proposed to play a role in coordinating neural communication (Fries, 2005; Canolty and Knight, 2010; Voytek et al., 2010a, 2013, 2015; van Der Meij et al., 2012). This phase/amplitude coupling (PAC) is quantified by examining the change in high gamma amplitude relative to the phase of a low-frequency oscillation. In essence, when a region is strongly phase/amplitude coupled, high gamma amplitude will be greater during some phase intervals and less during others. By definition, if more neurons are spiking in a more temporally random manner, population spiking will be more random relative to the dominant oscillatory mode, resulting in decreased PAC. Given that PAC plays such an important role in cognitive functioning and interregional neuronal communication (Voytek et al., 2015), we hypothesize that increased 1/*f* noise would similarly result in cognitive impairments (Voytek and Knight, 2015).

Materials and Methods

All data were analyzed in MATLAB (R2013b, Natick, MA) using custom scripts.

Electrocorticography (ECoG) data collection. Data were collected from 15 patients with intractable epilepsy (4 female; 11 male) who were implanted with chronic subdural electrodes, the placement of which was determined by surgeons based solely on the clinical needs of each patient as part of a preoperative procedure to localize the epileptogenic focus. Data were recorded at three hospitals: the Stanford School of Medicine, the Johns Hopkins School of Medicine, or the University of California, San Francisco. All participants gave written informed consent to participate in the study in accordance with the procedures and review boards established at each hospital and at the University of California Berkeley.

ECoG data were amplified ×10,000, analog filtered (0.01–1000 Hz), digitized, and downsampled to 1000 Hz. Data were rereferenced to the common average off-line to avoid spatial bias due to the choice of intracranial reference electrode (Boatman-Reich et al., 2010), high-pass filtered above 1.0 Hz with a symmetrical (phase true) finite impulse response filter (~35 dB/octave roll-off). Channels with low signal-to-noise ratio were identified and removed from analyses (i.e., 60 Hz line interference, electromagnetic noise from hospital equipment, amplifier saturation, and/or poor contact with cortical surface). Epileptic channels and epochs with seizure spread were also removed from analysis.

Only data from frontal, temporal, and supramarginal neocortical regions during blocks where participants performed listening tasks were included in analyses. These criteria were chosen based upon single-unit data suggesting that neural noise increases in rat auditory cortical neurons with age (Turner et al., 2005; de Villers-Sidani et al., 2010) and from human ECoG findings suggesting that theta/high gamma coupling is dominant in frontal and temporal neocortical regions during auditory tasks (Voytek et al., 2010a).

EEG participants. All participants gave informed consent approved by the University of California Berkeley Committee on Human Research. EEG data were collected from 11 younger (20–30 years old; 7 female; 4 male) and 13 older (60–70 years old; 5 female; 8 male) adults using a BioSemi ActiveTwo 64-channel DC amplifier with 24-bit resolution, sampled at 1024 Hz. All subjects performed a visual working memory paradigm (Voytek and Knight, 2010). Briefly, subjects were visually presented with one, two, or three lateralized colored squares for 180 ms; these squares only appeared in one visual hemifield at a time. After a 900 ms delay, a test array of the same number of colored squares appeared in the same spatial location. Subjects were instructed to manually respond to indicate whether or not the test array was the same color as the initial memory array.

Behavioral accuracy was assessed using a d′ measure of sensitivity, which takes into account false alarm rate to correct for response bias. To avoid mathematical constraints in the calculation of d′, we applied a standard correction procedure wherein, for any subjects with a 100% hit rate or 0% false alarm rate, performance was adjusted such that $1/(2N)$ false alarms were added or $1/(2N)$ hits subtracted where necessary (where N indicates number of trials per subject). All behavioral measures are the average performance across all three memory loads.

Power spectral density (PSD). PSD was estimated using Welch's method wherein the PSD was estimated for each channel separately using N 2 s time windows with 50% overlap where the data time-series, g, were multiplied by a 2 s Hamming window w giving g'. For EEG analyses, any window containing eye blink or eye movement artifacts (as identified from the ocular electrodes) were not included in the PSD estimate. PSD is defined such that,

$$PSD = \log_{10}\left(N^{-1}\sum_{n=1}^{N} 2\tilde{g}_i'^2\right), \quad (1)$$

where $\tilde{g}_i'$ is the discrete Fourier transformation of g_i'. The slope of the power spectrum (ν_n) was estimated using a linear regression approach in semi-log space where the power P at each discrete frequency f was estimated from the frequency itself from the following:

$$P_f = f'\beta + \varepsilon, \quad (2)$$

where f' is a two-column matrix composed of the discrete frequencies of the bands of interest and a column of ones; β is the regression coefficient (the slope of the model), and ε is the error term. The shape of the ECoG and EEG power spectra are such that β is typically negative. The slope of the PSD is different from the power. This is important given that task-related increases in neural activity result in an overall increase, an upward shift, in the broadband and high gamma PSD (Manning et al., 2009; Miller et al., 2009b).

Because scalp EEG poses unique problems with high-frequency (>40 Hz) noise from multiple non-neural sources, including scalp and eye muscles (Yuval-Greenberg et al., 2008; Voytek et al., 2010b) and has a lower noise floor compared with ECoG, these factors limit the ability to estimate of the high gamma slope and preclude high gamma-based PAC analyses. Although the ECoG results suggest that the high gamma power range provides a sensitive estimate of small changes in spectral slope,

theoretically, if the 1/*f* noise is great enough, noise-related changes in the slope of the power spectrum should be evident even at lower frequencies, providing a means for observing slope changes using scalp EEG. Therefore, for scalp EEG participants, slope was estimated not from the high gamma range, but from the (2–24 Hz) PSD, excluding power from visual cortical alpha (7–14 Hz), which represents nonbroadband oscillations and is thus not suitable for including in an estimate of broadband spectral slope (Miller et al., 2009a).

Phase/amplitude coupling. To compute the comodulogram (see Fig. 2*D*), the data for each channel were first filtered in the theta range using a two-way, zero phase-lag, finite impulse response filter (*eegfilt.m* function in EEGLAB) to prevent phase distortion. The filter order is defined as 3*r* where *r* is the ratio of the sampling rate to the low-frequency cutoff of the filter, rounded down. We then applied a Hilbert transform (*hilbert.m* function in MATLAB, The MathWorks) to construct a complex valued time-series as follows:

$$h_\theta[n] = \alpha_\theta[n] e^{i\phi_\theta[n]}, \quad (3)$$

where $a_\theta[n]$ and $\phi_\theta[n]$ are the analytic amplitudes and phases, respectively, of the theta passband. The Hilbert phase and amplitude estimation method yields results equivalent to sliding window FFT and wavelet approaches (Bruns, 2004). The phase time-series ϕ assumes values within $(-\pi, \pi]$ radians with a cosine phase such that $\pm\pi$ radians correspond to the troughs and 0 radians to the peak. Theta troughs were identified from the local minima of ϕ_θ using a window of ±5% of the theta cycle, and these troughs were used as time-locking events with a window of ±500 ms around the trough. These theta-phase-determined event times were then used to create event-related spectra perturbation plots. To calculate the event-related spectra perturbation, the ECoG data were first filtered into separate, partially overlapping, logarithmically-spaced passbands *f* with a 2 Hz bandwidth with center frequencies from 4 to 250 Hz. We seeded the first pass band such that $f_{p(n)} = [f_{L(n)}\, f_{H(n)}]$; where for $n = 1$, $f_{L(n)} = 0.5$, and $f_{H(n)} = 0.9$. Successive bands were calculated such that $f_{L(n)} = 0.85(f_{H(n-1)})$ and $f_{H(n)} = 1.1 + (f_{H(n-1)} - f_{L(n-1)})f_{L(n)}$. The analytic amplitude (the absolute value, or modulus, of h_f) a_f for each passband *f* was estimated using the Hilbert transform, normalized by its *z*-score as follows:

$$z_f = \sigma_f^{-1}(\alpha_f - \mu_f), \quad (4)$$

where μ_f is the mean of a_f, and σ_f is its SD. From this time series, the average amplitude of each passband around the theta trough was calculated.

PAC for each ECoG participant was calculated from 1000 randomly sampled 10 s segments of data collected while the participants were performing the auditory tasks, sampling equally from all channels and trials included in the analysis. To get an estimate of the age/PAC correlation error, 100 pulls of 1000 data segments were performed (see Fig. 2*F*); however, the error around the PAC estimate was very low. Theta/high gamma PAC was calculated by first filtering the data in separate theta (4–8 Hz) and high gamma (80–150 Hz) bands and extracting the analytic theta phase (ϕ_θ) and analytic high gamma amplitude (a_γ) time series. A second bandpass filter was then applied to a_γ using the same filter parameters used to extract ϕ_θ, resulting in a new time series, $a_{\gamma\theta}$. A second Hilbert transform is then used to extract the phases of the theta-filtered high gamma amplitude envelope as follows:

$$h_{a_{\gamma^\theta}}[n] = a_{a_{\gamma^\theta}}[n] e^{i\phi_{a_{\gamma^\theta}}[n]}. \quad (5)$$

PAC between theta and high gamma is defined as the length of the mean vector between ϕ_θ and $\phi_{\alpha_{\gamma^\theta}}$ using the following method (Penny et al., 2008):

$$PAC_{\theta\gamma} = N^{-1}\left|\sum_{n=1}^{N} e^{i(\phi_\theta[n] - \phi_{a_{\gamma^\theta}}[n])}\right|. \quad (6)$$

This gives a PAC estimate from [0,1] wherein a $PAC_{\theta\gamma}$ of 0 means that knowledge of the theta phase provides no information about high gamma amplitude, whereas a $PAC_{\theta\gamma}$ of 1 means that high gamma amplitude can be perfectly predicted from the theta phase. This measure is particularly sensitive to the level of noise (Tort et al., 2010) and is thus ideal for our use case. To test the specificity of the PAC results, a range of phase predictors were used to calculate PAC with high gamma amplitude. These phase predictors had partially overlapping 2 Hz passband center frequencies from 2 to 40 Hz, in steps of 1 Hz.

Results

ECoG results

We analyzed frontal and temporal cortical intracranial ECoG data collected from 15 participants spanning 38 years of age (Fig. 1), who performed auditory passive phoneme listening, word repetition, or auditory attention tasks (see Materials and Methods). These intracranial voltage recordings provided a means to assess local population spiking activity in the human brain with minimal contamination from non-neural sources (Voytek et al., 2010b). Specifically, high gamma power in direct neocortical recordings (usually in the range of 5–10 μV) correlates with neural spiking (Mukamel et al., 2005; Cardin et al., 2009).

Consistent with the neural noise hypothesis of aging, increased age is associated with a flatter, less negatively sloped high gamma power spectrum, such that the slope of high gamma power increases with age ($r = 0.50$, $p = 0.027$, one-tailed) (Fig. 2*A*,*B*). This effect remains significant after removing (partialling out) the effect of high gamma power ($r = 0.56$, $p = 0.018$, one-tailed), and high gamma power is uncorrelated with age ($r = -0.041$, $p = 0.44$, one-tailed) (Fig. 2*C*), supporting a dissociation between absolute high gamma power and the estimation of 1/*f* noise from the high gamma power spectral slope (Podvalny et al., 2015). In addition, aging was also associated with decreased theta/high gamma PAC ($r = -0.70$, $p = 0.002$, one-tailed) (Fig. 2*D*,*E*), and this effect remained significant after removing the effect of power in the theta ($r = -0.62$, $p = 0.009$, one-tailed) or high gamma ranges ($r = -0.71$, $p = 0.002$, one-tailed). These two empirically measured variables (slope of the power spectrum and theta/high gamma PAC) account for 60% of the variance in age (regression model, $R^2 = 0.60$, $p = 0.004$). To examine the specificity of the aging effect for theta/high gamma PAC, we calculated the correlation between age and the coupling of phase with high gamma power across other phase-providing oscillatory bands (1–40 Hz, 2 Hz bandwidth, 1 Hz steps). A *post hoc* analysis of the specificity of this age/PAC effect shows that age-related changes in PAC were restricted to the theta range ($p > 0.05$, all non-theta frequencies) (Fig. 2*F*).

Although these results are encouraging, there are several caveats associated with these ECoG data. First, these ECoG data were collected from participants with intractable epilepsy. Great care was taken to remove data contaminated by ictal spiking activity: channels with spread of seizure activity were identified by a neurologist or epileptologist and, along with electrodes over sites that were later surgically resected, were excluded from analysis. We also note that the older participants have had epilepsy for a longer time, which may lead to long-term neurophysiological changes that might also affect the results. Second, even though filter settings and digitization parameters were similar across sites, differences in the amplifier and recording systems may have impacted the results. We attempted to control for this effect by including recording location as a covariate in the analyses, none of which impacted the significant relationship between age and spectral slope ($p < 0.05$ correlation after regressing out each separate covariate).

Electroencephalographic results

To address the potential confounds that arose from the constraints of the ECoG recording environment, and to better exam-

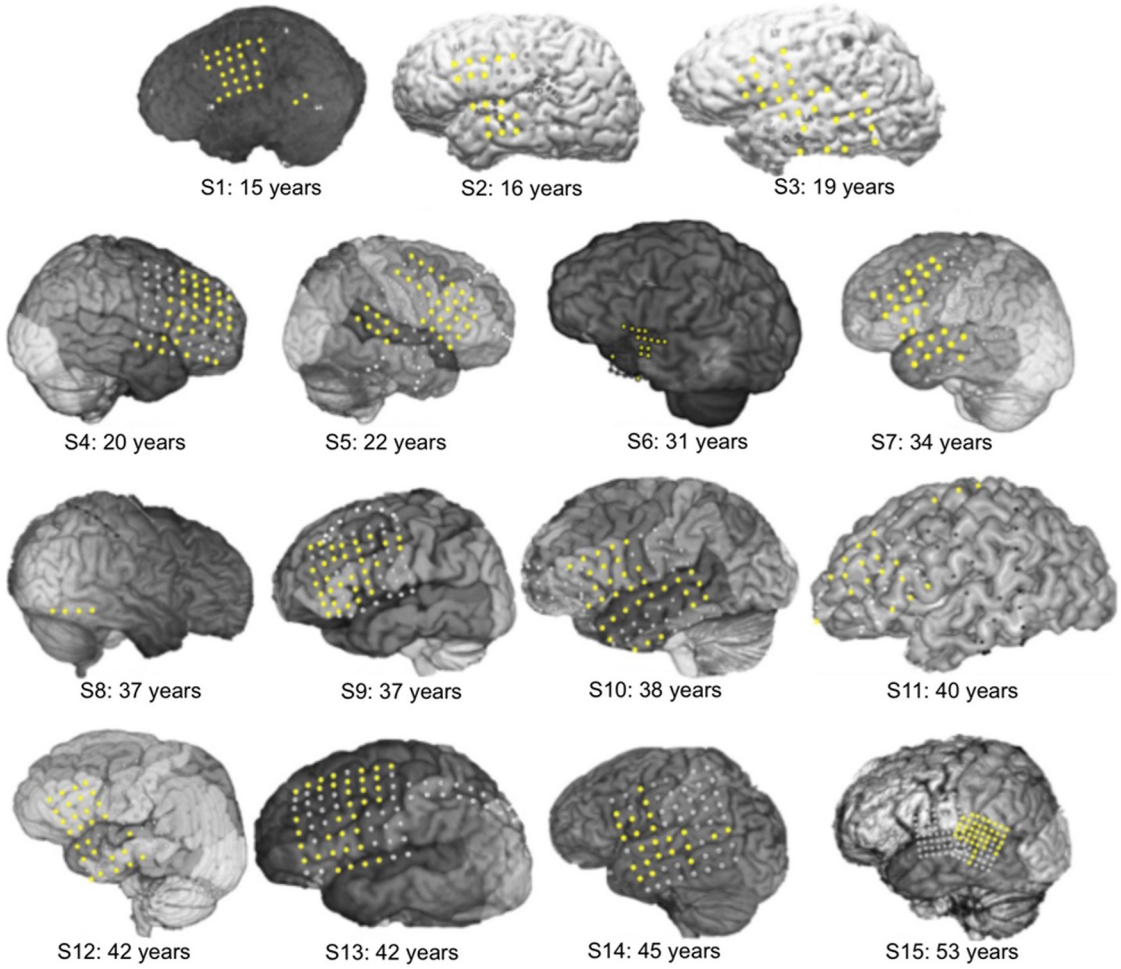

Figure 1. Electrode locations for research participants. Intracranial ECoG data were collected from 15 participants (15–53 years of age) performing auditory tasks. Data from artifact-free frontotemporal neocortical sites (yellow electrodes) were included in the analyses.

ine the relationship between behavior and 1/*f* noise, we collected noninvasive scalp EEG from a group of healthy younger (20–30 years old, $n = 11$) and older (60–70 years old, $n = 13$) adults. All EEG data were recorded using the same amplifier in the same recording environment, thus minimizing possible confounds associated with recording system heterogeneity on 1/*f* noise estimates. Both groups performed a lateralized visual working memory task (Voytek and Knight, 2010) during EEG data collection (see Materials and Methods). Consistent with previous reports of age-related working memory impairments, aging was associated with decreased visual working memory performance (d′: $r = -0.57$, $p = 0.0035$) as well as with slower RTs ($r = 0.79$, $p < 10^{-5}$) and more variable RTs (RT_{std}: $r = 0.73$, $p < 10^{-4}$) (Fig. 3*A–C*).

The low-frequency human electrophysiological power spectrum is dominated by non-broadband, high-power oscillatory sources (Miller et al., 2009a, 2014). Furthermore, high-frequency power is more difficult to interpret in the scalp EEG due to large, non-neural artifacts from (e.g., saccades) (Yuval-Greenberg et al., 2008) and scalp muscles (Voytek et al., 2010b). To avoid these potential confounds, we focused on the slope of the power spectrum across a low-frequency range (2–24 Hz), excluding a 7–14 Hz alpha buffer segment to mitigate the impact of this high-power, non-broadband spectral peak on estimates of the broadband slope (Fig. 3*D*). As reported previously (Polich, 1997), aging was associated with decreased power in the theta and alpha (4–14 Hz) ranges ($r = 0.79$, $p < 10^{-5}$).

To assess the impact of 1/*f* noise on this low-frequency range, we first analyzed the correlation between age and the low-frequency spectral slope (2–24 Hz) in the ECoG data (2–24 Hz, excluding 7–14 Hz). We find similar results as for the high-frequency spectral slope: as age increases, the low-frequency ECoG spectral slope also flattens ($r = 0.63$, $p = 0.006$, one-tailed, excluding 4–8 Hz theta). In agreement with these ECoG results, we also observe a significant correlation between age and low-frequency spectral slope in the EEG cohort ($r = 0.70$, $p = 0.00013$) (Fig. 3*E*). Although this a priori analysis focused on visual extrastriate 1/*f* noise, scalp topographic correlation analyses reveal that 1/*f* noise over central-parietal ($r = 0.66$, $p = 0.0004$) and frontal midline scalp sites ($r = 0.67$, $p = 0.0003$) also increases as a function of age (Fig. 3*F*).

Importantly, we also found that visual cortical 1/*f* noise was predictive of decreased working memory performance ($r = -0.50$, $p = 0.014$) and slower ($r = 0.63$, $p = 0.001$) and more variable RTs ($r = 0.50$, $p = 0.014$) (Fig. 4). We performed mediation analyses to assess the impact of visual cortical 1/*f* noise on the relationship between aging and the three behavioral measures (accuracy, RT, and RT variability) (Fig. 4, bottom). When visual cortical 1/*f* noise is accounted for in the mediation analysis, the relationship between age and accuracy becomes insignificant (from $r = -0.57$, $p = 0.0035$ to

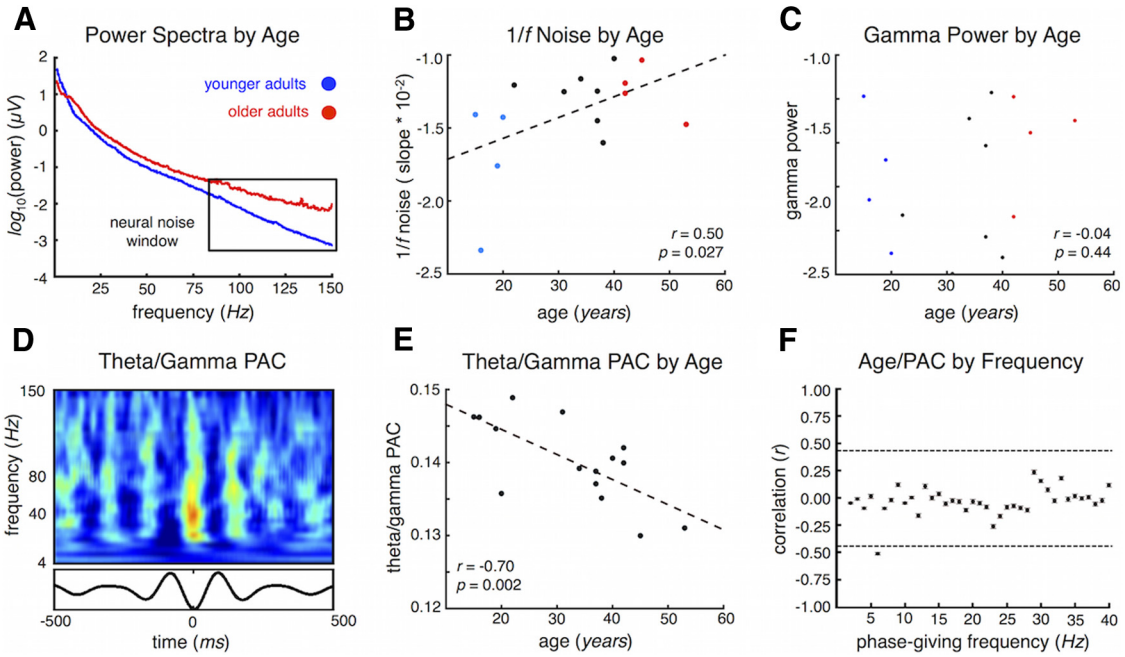

Figure 2. ECoG results. ***A***, Averaging power spectra by adults younger than 21 years (blue) and older than 40 years (red) illustrates the differences in the slope of high gamma power (outlined by the black box); the high-frequency power "flattens out," indicative of increased 1/*f* noise. ***B***, Experimental results showing that, with increasing participant age, there is increased 1/*f* noise without (***C***) a concomitant age-related increase in gamma power. Blue and red dots represent the subjects averaged in ***A***. ***D***, Example PAC comodulogram from one participant showing the relationship between theta phase (4 – 8 Hz, bottom oscillation) and amplitude at frequencies from 4 to 150 Hz. ***E***, Experimental results showing that theta/high gamma PAC decreases as a function of participant age. ***F***, Age-related changes in frontal and auditory PAC are specific to theta/high gamma PAC, as opposed to other phase-giving frequency bands. Dashed lines in ***F*** indicate significance cutoff ($p < 0.05$, uncorrected). Error bars indicate SEM.

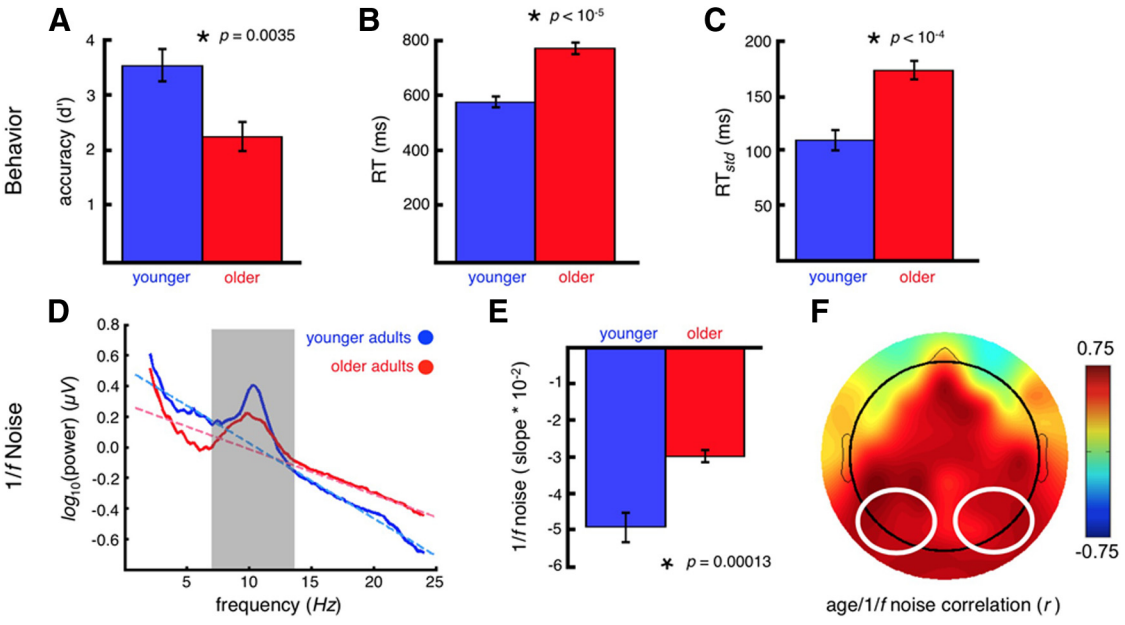

Figure 3. Behavioral and EEG results. In a visual working memory task, compared with younger adults (blue), older adults (red) are less accurate (***A***) and respond more slowly (***B***), with more variability (***C***). ***D***, The slope of the low-frequency power spectrum in the a priori visual cortical region of interest (***F***, white outline) is flatter in older adults compared with younger adults. 1/*f* noise is estimated from the slope of the power spectrum (dashed lines), ignoring alpha oscillatory power (shaded region, 7–14 Hz). ***E***, Older adults have more visual cortical 1/*f* noise compared with younger adults. ***F***, This effect is most prominent in visual extrastriate, parietal, and midline frontal cortex. Error bars indicate SEM.

$r = -0.36, p = 0.091$). That is, although age appears to explain 33% of the variance in behavioral accuracy, this effect appears to be largely statistically mediated by age-related increases in 1/*f* noise. Removing visual 1/*f* noise variance from the relationship between age and behavioral accuracy drops the proportion of explained variance by 20% to 13%. In contrast, removing visual cortical 1/*f* noise variance from the relationship between age and RT or RT variance had no effect on their respective significances ($p < 0.01$, both). Interestingly, removing 1/*f* noise from the motor cortical regions contralateral to the response hand, or from midline frontal regions, also had no effect on the significant relationship between age and RT or RT variance ($p < 0.01$, both).

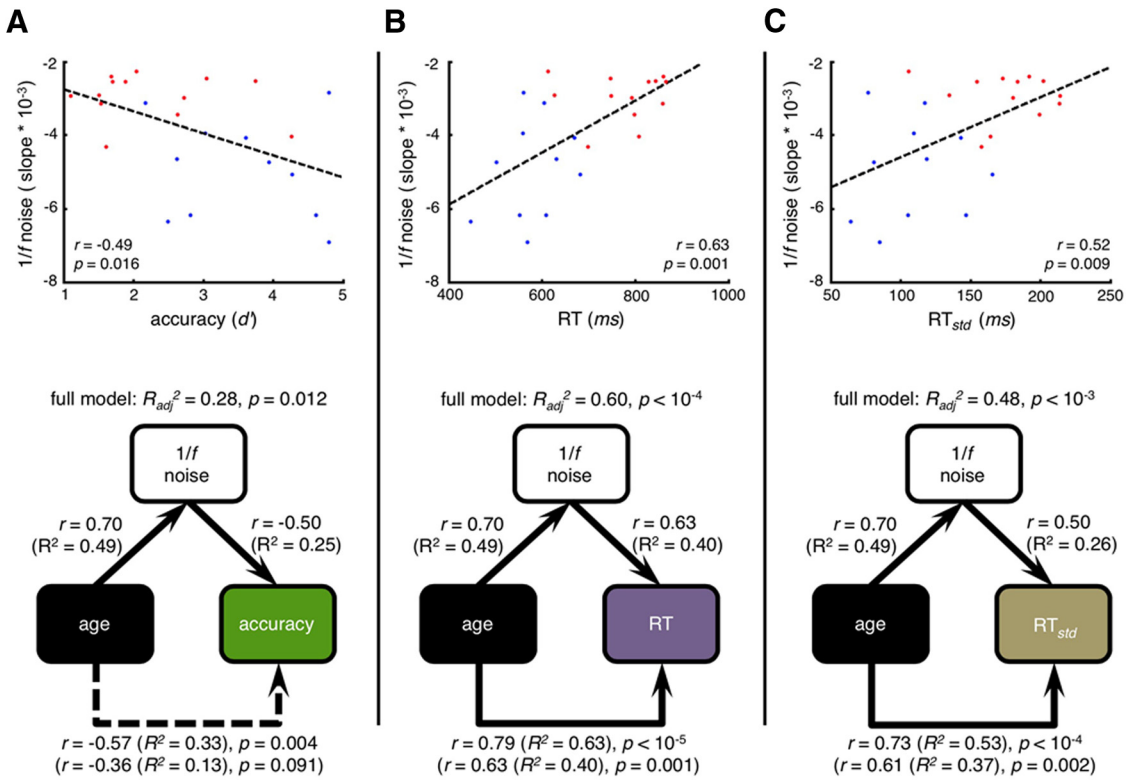

Figure 4. 1/*f* noise and behavior. ***A***, Greater visual cortical 1/*f* noise across younger (blue) and older (red) adults predicts lower working memory performance (top). Mediation analyses (bottom) shows that visual cortical 1/*f* noise statistically mediates age-related visual working memory decline. Although aging is associated with both increased 1/*f* noise and decreased visual working memory accuracy, and visual cortical 1/*f* noise predicts accuracy impairments, the relationship between age and accuracy became insignificant after including 1/*f* noise in the model (bottom *r*/*p* value pairs). 1/*f* noise is also associated with longer RTs (***B***) and greater RT variability (***C***); however, it does not act as a mediating variable for either of these RT measures.

Discussion

These convergent results across invasive and noninvasive human electrophysiology provide strong evidence that aging results in increased 1/*f* noise in humans. Moreover, the EEG data revealed a relationship between a marker of neural noise and cognitive performance. Overall, these results form a general framework that links aging, neural noise, oscillatory brain voltage dynamics, and behavior. It is important to note that, whereas most studies on neural noise in aging operationalize noise as either behavioral or neural activity variability, the main marker of neural noise used in this manuscript is a signal processing definition based on the shape of the PSD. By definition, white noise is a stochastic signal with equal, positive power at all frequencies, whereas 1/*f* noise, as seen in human EEG, ECoG, fMRI, and even behavioral processes (Gilden et al., 1995), arises due to the presence of temporal correlations within the data (although the nature of the underlying process giving rise to this phenomenon remains in contention) (Wagenmakers et al., 2005).

Decades of human behavioral and neuroimaging evidence suggest that neural noise increases with age, but these studies have relied upon proxies for neural noise. One such proxy is behavioral RT, the use of which is predicated on the inference that a noisier brain would have greater behavioral variability and slower information processing (Welford, 1981; Salthouse and Lichty, 1985). fMRI studies define noise as signal variability (Aguirre et al., 1998; D'Esposito et al., 1999; Huettel et al., 2001) or related information theoretic measures (McIntosh et al., 2008). However, the variability definition of noise may be problematic given that trial-by-trial variability need not arise from noise per se but rather may represent shifts in cognitive strategy and/or represent an adaptive neural mechanism underlying behavioral plasticity with aging (Ghosh et al., 2008; Garrett et al., 2010, 2013). Defining neural noise is further complicated by the fact that it is difficult to distinguish noise from true signal in neural activity (Pinneo, 1966; Faisal et al., 2008).

The scalp EEG spectral findings show a flattening of the slope with decreases in power from 8 to 14 Hz and increases between 14 and 25 Hz. These results have been previously observed (Polich, 1997) without a contextual interpretation of changes in spectral slope. The ECoG data show that gamma activity increases with age, providing further evidence for age-related flattening of the power spectrum (Hong and Rebec, 2012). We argue that, by considering the entire power spectrum as a unified statistical representation of the signal rather than examining semiarbitrary frequency sub-bands, age-related low-frequency power decreases and high-frequency power increases underlie the same phenomenon: increased 1/*f* noise causing a flattening of the power spectrum (Voytek and Knight, 2015).

The PSD can be represented as the mixture of several processes, namely, the 1/*f* noise component and any narrowband oscillations present in the signal as well (Podvalny et al., 2015; Voytek and Knight, 2015). The 1/*f* component itself reflects a total offset (the broadband power) and the slope. Recent findings provide evidence that the broadband power reflects the aggregate spiking activity of the underlying neuronal popula-

tion (Manning et al., 2009; Miller et al., 2009a, 2014). Computational work shows that the slope of the PSD flattens when the populating spiking activity is decoupled from an oscillatory regimen (Freeman and Zhai, 2009; Voytek and Knight, 2015). This effect may be driven by increases in the local excitation/inhibition ratio, which has been defined more broadly as "noise" (Rubenstein and Merzenich, 2003). Additionally, recent evidence has found that ECoG PSD slope changes with behavioral state (Podvalny et al., 2015). These slope changes are interpreted as possible changes in the temporal correlation of the underlying neuronal population, consistent with the hypothetical framework presented herein, as well as with previous reports (Usher et al., 1995; Pozzorini et al., 2013; Gao, 2015; Voytek and Knight, 2015). Of note is the observation that, in some neural populations, changes in 1/*f* slope are correlated with band-limited gamma activity, although this effect may be more restricted to visual cortical populations (Hermes et al., 2015; Podvalny et al., 2015). Although we restricted our ECoG analyses to frontotemporal populations, we controlled for overall high gamma power, which did not affect the observed relationship between age and 1/*f* slope. Furthermore, we observe a striking specificity of the age/PAC relationship limited to the theta band (Fig. 2*F*), with no effect in other frequencies. This is likely due to our use of a narrower bandwidth (2 Hz) for the full *post hoc* analysis of the full spectrum, as opposed to the 4 Hz a priori theta band analysis. Such narrowband theta effects in the human neocortex are not without precedent, with interelectrode phase locking during listening/word processing across even long cortical distances significantly higher for narrowband theta compared with even nearby frequencies (Canolty et al., 2007; compared their Fig. 8*A*).

The EEG results suggest that age-related changes in visual cortical 1/*f* noise are associated with cognitive decline. It is important to note that this effect occurred in a specific working memory task. Interestingly, whereas many studies examining the neural noise hypothesis of aging use RT variability as a proxy metric for neural noise, our mediation analyses suggest that visual cortical, motor cortical, or frontocentral 1/*f* noise does not contribute substantially to age-related RT variability, but rather 1/*f* noise statistically mediates the relationship between age and visual working memory decline. Here, mediation means that the relationship between aging and working memory decline is reduced when 1/*f* noise is taken into account, which suggests that the observed correlation between aging and working memory decline is partially driven by age-related changes in 1/*f* noise. This finding is parsimonious with prior fMRI work showing that aging and signal variability mediate an age-related behavioral impairment in financial risk-taking (Samanez-Larkin et al., 2010).

Our results stand in contrast to other studies that use different metrics of noise. Both interindividual and intraindividual behavioral variability has been shown to correlate with structural, functional, and neuromodulatory systems (Macdonald et al., 2006). For example, reductions in frontocentral theta intertrial phase coherence, a measure of phase consistency that decreases with increasing phase noise, are predictive of increased RT variability across the lifespan (Papenberg et al., 2013). RT variability has also been shown to increase with decreased dopamine binding potential across frontal and parietal cortices, the cortical distribution of which differs with aging (MacDonald et al., 2012). Both of those experiments, however, made use of tasks without delay periods, substantially different from the visual working memory task used in our experiment. Although we focus on the potential detriments of 1/*f* noise, in certain cases noise plays an important role in the CNS and may actually improve signal detection in some situations with weak stimuli via stochastic resonance (Li et al., 2006b; McDonnell and Abbott, 2009). Previous neurocomputational models show that increased noise in aging is associated with deficits in neuromodulatory systems, leading to diminished neuroplasticity (Li et al., 2006a) and reduced efficacy of stochastic resonance for stimulus detection (Li et al., 2006b). The method of estimating neural noise used here is computationally efficient and easily estimated from scalp EEG, making it useful for studying the effects of noise on cognitive functioning and in disease states associated with increased noise, such as autism and other neuropsychiatric disorders (Dinstein et al., 2012; Voytek and Knight, 2015).

Understanding the basic neurophysiology underlying age-related cognitive decline is an emerging public health issue. The world's population is rapidly aging: adults 55 years or older are the fastest growing population in the labor market (Toossi, 2012). Combating cognitive decline will require an increased understanding of the fundamental anatomy and physiology of aging. Here, through the use of a general neurocomputational framework, neural electrophysiology is linked to age-related cognitive decline. Given that cognitive decline is considered the most disabling consequence of aging (Bayles et al., 1987), insights into the biological basis of age-related cognitive decline provides new possibilities for improving the quality of life in an increasingly aging world. In addition to revealing a neurophysiological correlate of cognitive deficits with aging, this approach may provide an estimator for exploring neural underpinnings of cognitive changes across a variety of disease states.

References

Aguirre GK, Zarahn E, D'Esposito M (1998) The variability of human, BOLD hemodynamic responses. Neuroimage 8:360–369. CrossRef Medline

Bayles KA, Kaszniak AW, Tomoeda CK (1987) Communication and cognition in normal aging and dementia. Boston, MA: Little, Brown and Company.

Bédard C, Kröger H, Destexhe A (2006) Does the 1/f frequency scaling of brain signals reflect self-organized critical states? Phys Rev Lett 97:118102. CrossRef Medline

Boatman-Reich D, Franaszczuk PJ, Korzeniewska A, Caffo B, Ritzl EK, Colwell S, Crone NE (2010) Quantifying auditory event-related responses in multichannel human intracranial recordings. Front Comput Neurosci 4:4. CrossRef Medline

Bruns A (2004) Fourier-, Hilbert- and wavelet-based signal analysis: are they really different approaches? J Neurosci Methods 137:321–332. CrossRef Medline

Canolty RT, Knight RT (2010) The functional role of cross-frequency coupling. Trends Cogn Sci 14:506–515. CrossRef Medline

Canolty RT, Edwards E, Dalal SS, Soltani M, Nagarajan SS, Kirsch HE, Berger MS, Barbaro NM, Knight RT (2006) High gamma power is phase-locked to theta oscillations in human neocortex. Science 313:1626–1628. CrossRef Medline

Canolty RT, Soltani M, Dalal SS, Edwards E, Dronkers NF, Nagarajan SS, Kirsch HE, Barbaro NM, Knight RT (2007) Spatiotemporal dynamics of word processing in the human brain. Front Neurosci 1:185–196. CrossRef Medline

Cardin JA, Carlén M, Meletis K, Knoblich U, Zhang F, Deisseroth K, Tsai LH, Moore CI (2009) Driving fast-spiking cells induces gamma rhythm and controls sensory responses. Nature 459:663–667. CrossRef Medline

Cremer R, Zeef EJ (1987) What kind of noise increases with age? J Gerontol 42:515–518. CrossRef Medline

D'Esposito M, Zarahn E, Aguirre GK, Rypma B (1999) The effect of normal aging on the coupling of neural activity to the bold hemodynamic response. Neuroimage 10:6–14. CrossRef Medline

de Villers-Sidani E, Alzghoul L, Zhou X, Simpson KL, Lin RC, Merzenich MM (2010) Recovery of functional and structural age-related changes in the rat primary auditory cortex with operant training. Proc Natl Acad Sci U S A 107:13900–13905. CrossRef Medline

Dinstein I, Heeger DJ, Lorenzi L, Minshew NJ, Malach R, Behrmann M (2012) Unreliable evoked responses in autism. Neuron 75:981–991. CrossRef Medline

Faisal AA, Selen LP, Wolpert DM (2008) Noise in the nervous system. Nat Rev Neurosci 9:292–303. CrossRef Medline

Freeman WJ, Zhai J (2009) Simulated power spectral density (PSD) of background electrocorticogram (ECoG). Cogn Neurodyn 3:97–103. CrossRef Medline

Fries P (2005) A mechanism for cognitive dynamics: neuronal communication through neuronal coherence. Trends Cogn Sci 9:474–480. CrossRef Medline

Fröhlich F, McCormick DA (2010) Endogenous electric fields may guide neocortical network activity. Neuron 67:129–143. CrossRef Medline

Gao R (2015) Interpreting the electrophysiological power spectrum. J Neurophysiol. Advance online publication. Retrieved Aug. 5, 2015. doi: 10.1152/jn.00722.2015. CrossRef Medline

Garrett DD, Kovacevic N, McIntosh AR, Grady CL (2010) Blood oxygen level-dependent signal variability is more than just noise. J Neurosci 30: 4914–4921. CrossRef Medline

Garrett DD, Samanez-Larkin GR, MacDonald SW, Lindenberger U, McIntosh AR, Grady CL (2013) Moment-to-moment brain signal variability: a next frontier in human brain mapping? Neurosci Biobehav Rev 37:610–624. CrossRef Medline

Gazzaley A, Cooney JW, Rissman J, D'Esposito M (2005) Top-down suppression deficit underlies working memory impairment in normal aging. Nat Neurosci 8:1298–1300. CrossRef Medline

Gazzaley A, Sheridan MA, Cooney JW, D'Esposito M (2007) Age-related deficits in component processes of working memory. Neuropsychology 21:532–539. CrossRef Medline

Ghosh A, Rho Y, McIntosh AR, Kotter R, Jirsa VK (2008) Noise during rest enables the exploration of the brain's dynamic repertoire. PLoS Comp Biol 4:e1000196. CrossRef Medline

Gilden DL, Thornton T, Mallon MW (1995) 1/f noise in human cognition. Science 267:1837–1839. CrossRef Medline

Hanggi P, Jung P (1995) Colored noise in dynamical systems. Adv Chem Phys 89:239–326.

He BJ (2014) Scale-free brain activity: past, present, and future. Trends Cogn Sci 18:480–487. CrossRef Medline

He BJ, Zempel JM, Snyder AZ, Raichle ME (2010) The temporal structures and functional significance of scale-free brain activity. Neuron 66:353–369. CrossRef Medline

Hermes D, Miller KJ, Wandell BA, Winawer J (2015) Gamma oscillations in visual cortex: the stimulus matters. Trends Cogn Sci 19:57–58. CrossRef Medline

Hong SL, Rebec GV (2012) A new perspective on behavioral inconsistency and neural noise in aging: compensatory speeding of neural communication. Front Aging Neurosci 4:27. CrossRef Medline

Huettel SA, Singerman JD, McCarthy G (2001) The effects of aging upon the hemodynamic response measured by functional MRI. Neuroimage 13:161–175. CrossRef Medline

Lepage KQ, Kramer MA, Eden UT (2011) The dependence of spike field coherence on expected intensity. Neural Comput 23:2209–2241. CrossRef Medline

Li SC, Brehmer Y, Shing YL, Werkle-Bergner M, Lindenberger U (2006a) Neuromodulation of associative and organizational plasticity across the life span: empirical evidence and neurocomputational modeling. Neurosci Biobehav Rev 30:775–790. CrossRef Medline

Li SC, Oertzen von T, Lindenberger U (2006b) A neurocomputational model of stochastic resonance and aging. Neurocomputing 69:1553–1560. CrossRef

Macdonald SW, Nyberg L, Bäckman L (2006) Intra-individual variability in behavior: links to brain structure, neurotransmission and neuronal activity. Trends Neurosci 29:474–480. CrossRef Medline

MacDonald SW, Karlsson S, Rieckmann A, Nyberg L, Bäckman L (2012) Aging-related increases in behavioral variability: relations to losses of dopamine D1 receptors. J Neurosci 32:8186–8191. CrossRef Medline

Manning JR, Jacobs J, Fried I, Kahana MJ (2009) Broadband shifts in local field potential power spectra are correlated with single-neuron spiking in humans. J Neurosci 29:13613–13620. CrossRef Medline

McDonnell MD, Abbott D (2009) What is stochastic resonance? Definitions, misconceptions, debates, and its relevance to biology. PLoS Comp Biol 5:e1000348. CrossRef Medline

McIntosh AR, Kovacevic N, Itier RJ (2008) Increased brain signal variability accompanies lower behavioral variability in development. PLoS Comp Biol 4:e1000106. CrossRef Medline

Miller KJ, Sorensen LB, Ojemann JG, den Nijs M (2009a) Power-law scaling in the brain surface electric potential. PLoS Comp Biol 5:e1000609. CrossRef Medline

Miller KJ, Zanos S, Fetz EE, den Nijs M, Ojemann JG (2009b) Decoupling the cortical power spectrum reveals real-time representation of individual finger movements in humans. J Neurosci 29:3132–3137. CrossRef Medline

Miller KJ, Honey CJ, Hermes D, Rao RP, denNijs M, Ojemann JG (2014) Broadband changes in the cortical surface potential track activation of functionally diverse neuronal populations. Neuroimage 85:711–720. CrossRef Medline

Montemurro MA, Rasch MJ, Murayama Y, Logothetis NK, Panzeri S (2008) Phase-of-firing coding of natural visual stimuli in primary visual cortex. Curr Biol 18:375–380. CrossRef Medline

Mukamel R, Gelbard H, Arieli A, Hasson U, Fried I, Malach R (2005) Coupling between neuronal firing, field potentials, and FMRI in human auditory cortex. Science 309:951–954. CrossRef Medline

Nyberg L, Lövdén M, Riklund K, Lindenberger U, Bäckman L (2012) Memory aging and brain maintenance. Trends Cogn Sci 16:292–305. CrossRef Medline

Osipova D, Hermes D, Jensen O (2008) Gamma power is phase-locked to posterior alpha activity. PLoS One 3:e3990. CrossRef Medline

Papenberg G, Hämmerer D, Müller V, Lindenberger U, Li SC (2013) Lower theta inter-trial phase coherence during performance monitoring is related to higher reaction time variability: a lifespan study. Neuroimage 83:912–920. CrossRef Medline

Penny WD, Duzel E, Miller KJ, Ojemann JG (2008) Testing for nested oscillation. J Neurosci Methods 174:50–61. CrossRef Medline

Pinneo LR (1966) On noise in the nervous system. Psychol Rev 73:242–247. CrossRef Medline

Podvalny E, Noy N, Harel M, Bickel S, Chechik G, Schroeder CE, Mehta AD, Tsodyks M, Malach R (2015) A unifying principle underlying the extracellular field potential spectral responses in the human cortex. J Neurophysiol 114:505–519. CrossRef Medline

Polich J (1997) EEG and ERP assessment of normal aging. Electroencephalogr Clin Neurophysiol 104:244–256. CrossRef Medline

Pozzorini C, Naud R, Mensi S, Gerstner W (2013) Temporal whitening by power-law adaptation in neocortical neurons. Nat Neurosci 16:942–948. CrossRef Medline

Rubenstein JL, Merzenich MM (2003) Model of autism: increased ratio of excitation/inhibition in key neural systems. Genes Brain Behav 2:255–267. CrossRef Medline

Salthouse TA (2010) Selective review of cognitive aging. J Int Neuropsychol Soc 16:754–760. CrossRef Medline

Salthouse TA, Lichty W (1985) Tests of the neural noise hypothesis of age-related cognitive change. J Gerontol 40:443–450. CrossRef Medline

Samanez-Larkin GR, Kuhnen CM, Yoo DJ, Knutson B (2010) Variability in nucleus accumbens activity mediates age-related suboptimal financial risk taking. J Neurosci 30:1426–1434. CrossRef Medline

Shannon C (1948) A mathematical theory of communication. Bell Syst Tech J 27:623–656. CrossRef

Sosnoff JJ, Newell KM (2011) Aging and motor variability: a test of the neural noise hypothesis. Exp Aging Res 37:377–397. CrossRef Medline

Toossi M (2012) Labor force projections to 2020: a more slowly growing workforce. Monthly Lab Rev 135:43.

Tort AB, Komorowski R, Eichenbaum H, Kopell N (2010) Measuring phase-amplitude coupling between neuronal oscillations of different frequencies. J Neurophysiol 104:1195–1210. CrossRef Medline

Turner JG, Hughes LF, Caspary DM (2005) Affects of aging on receptive fields in rat primary auditory cortex layer V neurons. J Neurophysiol 94:2738–2747. CrossRef Medline

Usher M, Stemmler M, Olami Z (1995) Dynamic pattern formation leads to 1f noise in neural populations. Phys Rev Lett 74:326–329. CrossRef Medline

van Der Meij R, Kahana M, Maris E (2012) Phase-amplitude coupling in

human electrocorticography is spatially distributed and phase diverse. J Neurosci 32:111–123. CrossRef Medline

Voytek B, Knight RT (2010) Prefrontal cortex and basal ganglia contributions to visual working memory. Proc Natl Acad Sci U S A 107:18167–18172. CrossRef Medline

Voytek B, Knight RT (2015) Dynamic network communication as a unifying neural basis for cognition, development, aging, and disease. Biol Psychiatry 77:1089–1097. CrossRef Medline

Voytek B, Canolty RT, Shestyuk A, Crone NE, Parvizi J, Knight RT (2010a) Shifts in gamma phase–amplitude coupling frequency from theta to alpha over posterior cortex during visual tasks. Front Hum Neurosci 4:191. CrossRef Medline

Voytek B, Secundo L, Bidet-Caulet A, Scabini D, Stiver SI, Gean AD, Manley GT, Knight RT (2010b) Hemicraniectomy: a new model for human electrophysiology with high spatio-temporal resolution. J Cogn Neurosci 22:2491–2502. CrossRef Medline

Voytek B, D'Esposito M, Crone N, Knight RT (2013) A method for event-related phase/amplitude coupling. Neuroimage 64:416–424. CrossRef Medline

Voytek B, Kayser AS, Badre D, Fegen D, Chang EF, Crone NE, Parvizi J, Knight RT, D'Esposito M (2015) Oscillatory dynamics coordinating human frontal networks in support of goal maintenance. Nat Neurosci 18:1318–1324. CrossRef Medline

Wagenmakers EJ, Farrell S, Ratcliff R (2005) Human cognition and a pile of sand: a discussion on serial correlations and self-organized criticality. J Exp Psychol Gen 134:108–116. CrossRef Medline

Welford AT (1981) Signal, noise, performance, and age. Hum Factors 23:97–109. CrossRef Medline

Yuval-Greenberg S, Tomer O, Keren AS, Nelken I, Deouell LY (2008) Transient induced gamma-band response in EEG as a manifestation of miniature saccades. Neuron 58:429–441. CrossRef Medline